J|A|C|S
ARTICLES
Published on Web 04/10/2003

Thermal and Electrochemical C−X Activation (X = Cl, Br, I) by the Strong Lewis Acid $Pd_3(dppm)_3(CO)^{2+}$ Cluster and Its Catalytic Applications

Frédéric Lemaître,[1a,b] Dominique Lucas,*[,1a] Katherine Groison,[1b] Philippe Richard,[1a] Yves Mugnier,[1a] and Pierre D. Harvey*[,1b]

Contribution from the Laboratoire de Synthèse et d'Electrosynthèse Organométalliques, CNRS UMR 5632, Faculté des Sciences Gabriel, Université de Bourgogne, 6 Boulevard Gabriel, 21000 Dijon, France and the Département de Chimie, Université de Sherbrooke, Sherbrooke, Québec, Canada J1K 2R1

Received December 17, 2002; E-mail: p.harvey@USherbrooke.ca; lucasd@u-bourgogne.fr

Abstract: The stoichiometric and catalytic activations of alkyl halides and acid chlorides by the unsatured $Pd_3(dppm)_3(CO)^{2+}$ cluster (Pd_3^{2+}) are investigated in detail. A series of alkyl halides (R−X; R = *t*-Bu, Et, Pr, Bu, allyl; X = Cl, Br, I) react slowly with Pd_3^{2+} to form the corresponding $Pd_3(X)^+$ adduct and "R^+". This activation can proceed much faster if it is electrochemically induced via the formation of the paramagnetic species Pd_3^+. The latter is the first confidently identified paramagnetic Pd cluster. The kinetic constants extracted from the evolution of the UV−vis spectra for the thermal activation, as well as the amount of electricity to bring the activation to completion for the electrochemically induced reactions, correlate the relative C−X bond strength and the steric factors. The highly reactive "R^+" species has been trapped using phenol to afford the corresponding ether. On the other hand, the acid chlorides react rapidly with Pd_3^{2+} where no induction is necessary. The analysis of the cyclic voltammograms (CV) establishes that a dissociative mechanism operates ($RCOCl \rightarrow RCO^+ + Cl^-$; R = *t*-Bu, Ph) prior to Cl^- scavenging by the Pd_3^{2+} species. For the other acid chlorides (R = *n*-C_6H_{13}, Me_2CH, Et, Me, Pr), a second associative process ($Pd_3^{2+} + RCOCl \rightarrow Pd_3^{2+}\cdots Cl(CO)(R)$) is seen. Addition of $Cu(NCMe)_4^+$ or Ag^+ leads to the abstraction of Cl^- from $Pd_3(Cl)^+$ to form Pd_3^{2+} and the insoluble MCl materials (M = Cu, Ag) allowing to regenerate the starting unsaturated cluster, where the precipitation of MX drives the reaction. By using a copper anode, the quasi-quantitative catalytic generation of the acylium ion ("RCO^+") operates cleanly and rapidly. The trapping of "RCO^+" with PF_6^- or BF_4^- leads to the corresponding acid fluorides and, with an alcohol (R′OH), to the corresponding ester catalytically, under mild conditions. Attempts were made to trap the key intermediates "$Pd_3(Cl)^+...M^+$" ($M^+ = Cu^+$, Ag^+), which was successfully performed for $Pd_3(ClAg)^{2+}$, as characterized by ^{31}P NMR, IR, and FAB mass spectrometry. During the course of this investigation, the rare case of PF_6^- hydrolysis has been observed, where the product $PF_2O_2^-$ anion is observed in the complex $Pd_3(PF_2O_2)^+$, where the substrate is well-located inside the cavity formed by the dppm-Ph groups above the unsatured face of the Pd_3^{2+} center. This work shows that Pd_3^{2+} is a stronger Lewis acid in CH_2Cl_2 and THF than $AlCl_3$, Ag^+, Cu^+, and Tl^+.

Introduction.

The C−X bond activation (X = Cl, Br, I) is one of the most basic processes for the functionalization of organic molecules.[2] Its importance and the number of applications are simply impressive, ranging from the simple nucleophilic substitution[3] to the Heck reaction.[4] Among the common methodologies known for C−X bond activation, the use of Lewis acids such as $AlCl_3$, Ag^+, Cu^+, and Tl^+ ions are popular and convenient.[5]

Recently, we reported the stoichiometric C−X bond activation (X = Br, I) of alkyl halides by the unsaturated 42-electron cluster $Pd_3(dppm)_3(CO)^{2+}$ (Pd_3^{2+}).[6] The originality stems, in part, from the fact that this process operates inside a cavity

(1) (a) Université de Bourgogne. (b) Université de Sherbrooke.
(2) (a) Kulawiec, R. J.; Crabtree, R. H. *Coord. Chem. Rev.* **1990**, *99*, 89. (b) Stille, J. K.; Kriesler, S. Y. L. *Acc. Chem. Res.* **1977**, *10*, 434. (c) Kochi, J. K. *Organometallic Mechanisms and Cata1ysis*; Academic Press: New York, 1978; p 156. (d) Abel, E. W.; Stone, F. G. A.; Wilkinson, G. *Comprehensive Organometallic Chemistry II*; Pergamon: Oxford, U.K., 1995; Vol. 12, p 161. (e) Collman, J. P.; Hegedus, L. S.; Norton, J. R. *Principles and Applications of Organotransition Metal Chemistry*; University Science Books: Mill Valley, CA, 1987. (f) Cornils, B.; Hermann, W. A. *Applied Homogeneous Catalysis with Organometallic Compounds*; Wiley: Weinheim, Germany, 1999. (g) Tsuji, J. *Transition Metal Reagents and Catalysts: Innovations in Organic Synthesis*; Wiley: Chichester, U.K., 2000.
(3) (a) Trost, B. *Comprehensive Organic Synthesis;* Pergamon Press: New York, 1991; Vol. 4, Chapter 2. (b) Stock, L. M. *Aromatic Substitution Reactions;* Prentice Hall: Englewood Cliffs, NJ, 1968. (c) Clark, J. H.; Wails, D.; Bastock, T. W. *Aromatic Fluorination*; CRC Press: Boca Raton, FL, 1996. (d) Carey, F. A.; Sundberg, R. J. *Advanced Organic Chemistry*; Plenum Press: New York, 1990; Vol. A, Chapter 5, p 257.
(4) Beletskaya, I. P.; Cheprakov, A. V. *Chem. Rev.* **2000**, *100*, 3009 and references therein.

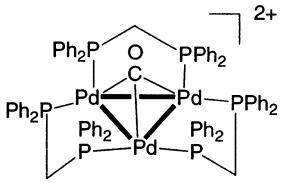

$Pd_3(dppm)_3(CO)^{2+}$

formed by the 6-dppm phenyl groups, above the Pd_3 triangular frame. The host−guest behavior for neutral species have been thoroughly investigated.[7] However, the C−X bond cleavage requires an electrochemical induction for the $[Pd_3(CF_3CO_2)](CF_3CO_2)$ species, provoking a change in oxidation state of Pd_3^{2+}, from $+^2/_3$ to $+^1/_3$. This change in the cluster charge induces a greater lability of the $CF_3CO_2^-$ ion, which is trapped in the cavity and attracted electrostatically by the positively charged Pd_3 center. Then, Pd_3^+ abstracts X^- from the R−X molecule. During the course of this research, we noticed that some R−X molecules slowly react with Pd_3^{2+} without the need of an electrochemical induction.

We now wish to report a full account on the reactivity of R−X molecules (X = Cl, Br, I; R = alkyl) and acid chlorides (R = alkyl, Ph) with Pd_3^{2+} on a mechanistic point of view and intermediate elucidation. In addition, an effort has been made to render this process catalytic and find new applications, notably for the electrosynthesis of acid fluorides and esters. The regeneration of the Pd_3^{2+} catalyst from the $Pd_3(X)^+$ species is also presented.

Experimental Section

Materials. $[Pd_3(dppm)_3(CO)](PF_6)_2$, $[Pd_3(dppm)_3(CO)(Cl)](PF_6)$, and $[Pd_3(dppm)_3(CO)(CF_3CO_2)](CF_3CO_2)$ have been prepared according to literature procedure.[8] Dichloromethane was distilled under Ar over P_2O_5, and tetrahydrofuran (THF) was distilled under Ar over Na (Aldrich). The acid chlorides and alcohols were purchased from Aldrich and used as received. The Bu_4NPF_6 salt was synthesized by mixing stoichiometric amounts of Bu_4NOH (40% in water) and HPF_6 (60% in water). After filtration, the salt was recrystallized twice in ethanol and dried at 80 °C for at least 2 days. Bu_4NBF_4, Bu_4NClO_4, and $NaBPh_4$ were purchased from Fluka (puriss p.a. for electrochemical grade) and used as received.

Apparatus. The UV−vis spectra were acquired on a Hewlett-Packard (HP 8452A) diode array spectrophotometer. NMR spectra were measured on a Bruker WM 300 spectrophotometer (^{1}H NMR, 300.15 MHz; ^{31}P NMR, 121.497 MHz). The reference was the residual nondeuterated solvent. The chemical shifts are reported with respect to TMS (^{1}H NMR) and H_3PO_4 (^{31}P NMR). The GC−MS data were collected on a Hewlett-Packard 6890 Series apparatus. EPR measurements were carried out on a Bruker ESP 300 spectrometer; field calibration was made with DPPH (g = 2.0037). Mass spectra were obtained with a Kratos Concept 32S spectrometer in the LSIMS mode (matrix = *m*-nitrobenzyl alcohol).

Electrochemical Experiments. All manipulations were performed using Schlenk techniques in an atmosphere of dry oxygen-free argon gas. The supporting electrolyte was degassed under vacuum before use and then solubilized at a concentration of 0.2 M. For cyclic voltammetry experiments, the concentration of the analyte was nearly 10^{-3} M. Voltammetric analyses were carried out in a standard three-electrode cell with a Tacussel PJT24-1 potentiostat connected to a waveform generator Tacussel GSTP4. The reference electrode was a saturated calomel electrode (SCE) separated from the solution by a sintered glass disk. The auxiliary electrode was a platinum wire. For all voltammetric measurements, the working electrode was a vitreous carbon electrode (ϕ = 3 mm). In these conditions, when operating in THF, the formal potential for the ferrocene$^{+/-}$ couple is found to be +0.56 V versus SCE. The controlled potential electrolysis was performed with an Amel 552 potentiostat coupled with an Amel 721 electronic integrator. High scale electrolyses were performed in a cell with three compartments separated with fritted glasses of medium porosity. A carbon gauze was used as the working electrode, a platinum plate, as the counter-electrode, and a saturated calomel electrode, as the reference electrode.

High scale electrolyses with acid chlorides were performed with a copper plate as the working electrode (anode), a platinum plate as the counter-electrode (cathode), and a saturated calomel electrode as the reference electrode, each one being separated from the others in a three-compartment cell (except the last experiment of Table 7 as described in the text).

Typical Procedures. Conversion of Acid Chlorides into Esters: Preparation of Ethyl Benzoate. The $[Pd_3(dppm)_3(CO)](PF_6)_2$ cluster (15.8 mg, 8.82×10^{-3} mmol, 1 mol %/mol of acyl chloride), ethanol (51 μL, 0.87 mmol), and benzoyl chloride (100 μL, 0.86 mmol) were added to the anodic compartment of the cell containing 15 mL of a 0.2 M solution of Bu_4NClO_4 in CH_2Cl_2. The cathodic compartment and the reference electrode compartment were filled with the Bu_4NClO_4−CH_2Cl_2 solution. The potential of the copper anode was set to +0.65 V versus SCE. The electrolysis was stopped after the current had dropped to less than 0.5 mA. After filtration of the mixture, the solvent was evaporated and the residue was extracted with ether (3 × 5 mL). The internal standard method was used to measure the GC yield of the ester product. The latter was identified by comparison of the GC−MS spectra and GC retention times to those of available authentic samples.

Fluorination of Acid Chlorides. The procedure is the same as described previously except that no alcohol is added and that Bu_4NPF_6 or Bu_4NBF_4 is used instead of Bu_4NClO_4.

Synthesis of $[Pd_3(dppm)_3(CO)(ClAg)](PF_6)_2$. To a solution of $[Pd_3(dppm)_3(CO)(Cl)](PF_6)$ (0.210 g, 0.125 mmol) in acetone (15 mL) was added $AgPF_6$ (7.52 mg, 0.137 mmol). The brown reaction mixture was allowed to stir at room temperature and became red. After 20 min, 3 mL of water were added and the solution was concentrated by the rotating evaporator. The resulting brown precipitate was isolated by filtration, washed 3 times with water, and dried with ether. Yield: 97%. ^{31}P NMR: $\delta(H_3PO_4)$ = −4.65 ppm (s). IR: ν(CO) = 1820 cm^{-1}. MS (FAB): *m*/*z* (fragment) = 659 (Pd_2(dppm)(Cl)(CO)); 734.7

(5) (a) Olah, G. A. *Friedel−Crafts Chemistry*; Wiley: New York, 1973. (b) Olah, G. A.; Krishnamurti, R.; Prakash, G. K. S. In *Comprehensive Organic Synthesis*; Trost, B. M., Ed.; Pergamon Press: Oxford, 1991; Vol. 3, Chapter 1.8, p 293. (c) Roberts, R. M.; Khalaf, A. A. *Friedel−Crafts Alkylation Chemistry*; Marcel Dekker: New York, 1984. (d) Klunder, J. M.; Posner, G. H. In *Comprehensive Organic Synthesis*; Trost, B. M., Fleming, I., Eds.; Pergamon Press: Elmsford, New York, 1991; Vol. 3, p 207. (e) Ingold, C. K. *Structure and Mechanism in Organic Chemistry*; Cornell University Press: Ithaca, New York, 1969. (f) Hartshorn, S. R. *Aliphatic Nucleophilic Substitution*; Cambridge University Press: London, 1973; p 20. (g) Lee, A. G. *The Chemistry of Thallium*; Elsevier: New York, 1971. (h) Herr, R. W.; Wieland, D. M.; Johnson, C. R. *J. Am. Chem. Soc.* **1970**, *92*, 3813. (i) Johnson, C. R.; Herr, R. W.; Wieland, D. M. *J. Org. Chem.* **1973**, *38*, 4263. (j) Johnson, C. R.; Dutra, G. A. *J. Am. Chem. Soc.* **1973**, *95*, 7783. (k) Lipshutz, B. H.; Wilhelm, R. S. *J. Am. Chem. Soc.* **1982**, *104*, 4696. Ashby, E. C.; Coleman, D. *J. Org. Chem.* **1987**, *52*, 4554. (l) Bertz, S. H.; Dabbagh, G.; Mujsce, A. M. *J. Am. Chem. Soc.* **1991**, *113*, 631.

(6) Brevet, D.; Lucas, D.; Cattey, H.; Lemaître, F.; Mugnier, Y.; Harvey, P. D. *J. Am. Chem. Soc.* **2001**, *123*, 4340.

(7) (a) Harvey, P. D.; Crozet, M.; Aye, K. T. *Can. J. Chem.* **1995**, *73*, 123. (b) Harvey, P. D.; Hubig, S.; Ziegler, T. *Inorg. Chem.* **1994**, *33*, 3700. (c) Harvey, P. D.; Provencher, R.; Gagnon, J.; Zhang, T.; Fortin, D.; Hierso, K.; Drouin, M.; Socol, S. M. *Can. J. Chem.* **1996**, *74*, 2268. (d) Provencher, R.; Aye, K. T.; Drouin, M.; Gagnon, J.; Boudreault, N.; Harvey, P. D. *Inorg. Chem.* **1994**, *33*, 3689.

(8) (a) Puddephatt, R. J.; Manojlovic-Muir, L.; Muir, K. W. *Polyhedron* **1990**, *9*, 2767 and references therein. (b) Manojlovic-Muir, L.; Muir, K. W.; Lloyd, B. R.; Puddephatt, R. J. *J. Chem. Soc., Chem. Commun.* **1983**, 1336. (c) Lloyd, R. J.; Manojlovic-Muir, L.; Muir, K. W.; Puddephatt, R. J. *Organometallics* **1993**, *12*, 1231. (d) Manojlovic-Muir, L.; Muir K. W.; Lloyd, B. R.; Puddephatt, R. J. *J. Chem. Soc., Chem. Commun.* **1985**, 536.

($Pd_3(dppm)_3$); 981.6 ($Pd_2(dppm)_2$); 1087.5 ($Pd_3(dppm)_2$); 1122 ($Pd_3(dppm)_2(Cl)$); 1395.4 ($Pd_2(dppm)_3(CO)$); 1470.4 ($Pd_3(dppm)_3$); 1499.4 ($Pd_3(dppm)_3(CO)$); 1612.3 ($Pd_3(dppm)_3(ClAg)$).

Crystallization from acetone/toluene/hexane superimposed layers leads to the isolation of two different crystalline phases, corresponding, respectively, to $[Pd_3(dppm)_3(CO)](PF_6)_2$ and $[Pd_3(dppm)_3(CO)(PO_2F_2)](PF_6)$.

Results and Discussion

$Pd_3(dppm)_3(CO)^+$ Species. Figure 1 shows the RDE voltammogram of Pd_3^{2+} (as a PF_6^- salt in THF/0.2M $NaBPh_4$; trace a) which exhibits two one-electron waves (based on coulometry)[9] at −0.29 V (A_1) and −0.66 V (A_2) versus SCE (−0.29 V (A_1) and −0.54 V (A_2) in THF/0.2M Bu_4NPF_6). The bulk electrolysis at wave A_1 generates a new product, which exhibits the RDE voltammogram shown in trace b. This species is the Pd_3^+ cluster. This same species can also be obtained by reducing Pd_3^{2+} at wave A_2 to generate Pd_3^0 (^{31}P NMR, δ(acetone-d_6) = 12 ppm). Then, the addition of 1 equiv of Tl^+ produces the monocation Pd_3^+ and metallic Tl (reaction 3). The $E_{1/2}^{0/+}$ of Tl is −0.582 V versus SCE, which indicates that this oxidation reaction is thermodynamically feasible.[10] Similarly, the bulk electrolysis at wave A_2 where only 1 equiv of electricity is passed through the solution generates Pd_3^+. Indeed, when applying this potential, Pd_3^0 is generated at the electrode. But the latter is unstable in the presence of unreduced Pd_3^{2+}, due to a fast compproponation equilibrium, strongly in favor of Pd_3^+ (reaction 5).

The three electrochemical methods are summarized in eqs 1−5: Method 1

$$Pd_3^{2+} + 1e^- \rightarrow Pd_3^+ \qquad \text{(wave } A_1\text{)} \qquad (1)$$

Method 2

$$Pd_3^{2+} + 2e^- \rightarrow Pd_3^0 \qquad \text{(wave } A_2\text{)} \qquad (2)$$

$$Pd_3^0 + Tl^+ \rightarrow Pd_3^+ + Tl(m) \qquad \text{(potentiostat off)} \qquad (3)$$

Method 3

$$Pd_3^{2+} + 1e^- \rightarrow {}^1/_2Pd_3^{2+} + {}^1/_2Pd_3^0 \qquad \text{(wave } A_2\text{)} \qquad (4)$$

$${}^1/_2Pd_3^{2+} + {}^1/_2Pd_3^0 \rightarrow Pd_3^+ \qquad \text{(potentiostat off)} \qquad (5)$$

Method 3 is preferred for a practical purpose: (i) It does not need the addition of an oxidation reagent as in method 2. (ii) Compared to method 1, by setting the potential at the potential of wave A_2 or lower, the duration of the electrolysis is significantly shortened.

For characterization purposes, this same 43-electron species can be cleanly chemically prepared using $NaBPh_4$ as reducing agent (eq 6):[11]

$$Pd_3^{2+} + NaBPh_4 \rightarrow Pd_3^+ + Na^+ + {}^1/_2Ph{-}Ph + BPh_3 \qquad (6)$$

where biphenyl is identified by GC−MS. The IR spectrum of Pd_3^+ exhibits a ν(CO) absorption at 1785 cm^{-1}, which is expectedly red-shifted in comparison with the more oxidized Pd_3^{2+} (ν(CO) = 1835 cm^{-1}) and blue-shifted with respect to the more reduced Pd_3^0 (ν(CO) = 1761 cm^{-1}),[9] due to the back-bonding effect.

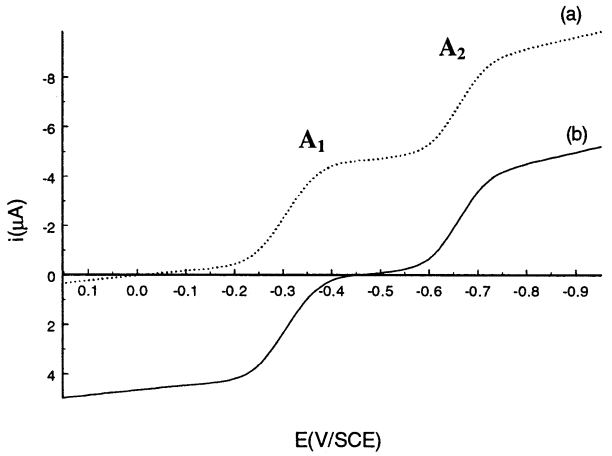

Figure 1. RDE voltammogram of 0.84 mM $Pd_3(PF_6)_2$, in THF. (a, dotted line) Alone; (b, solid line) after reduction with 0.2 M $NaBPh_4$. Initial potential: +0.2 V. Scan rate: 20 mV s^{-1}.

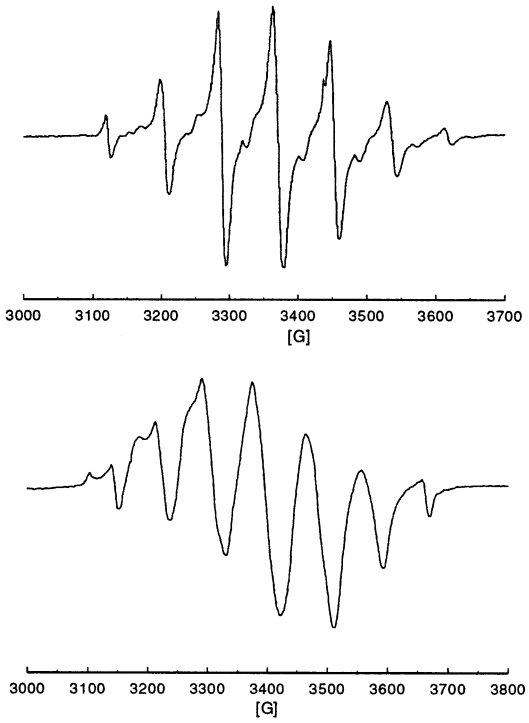

Figure 2. Experimental EPR spectrum of Pd_3^+ in THF at 293 K (top); experimental EPR spectrum of Pd_3^+ in THF at 100 K (bottom).

The isotropic (at 293 K) and anisotropic (at 100 K) EPR spectra for Pd_3^+ in THF were measured (Figure 2 as an example). The former exhibits a septet with a relative intensity approaching 1:6:15:20:15:6:1, along with a weaker structure. These are due to coupling with six equivalent P atoms ($S = {}^1/_2$; natural abundance ^{31}P 100%), hence demonstrating the presence of delocalization. This room-temperature spectrum also exhibits weaker signals beside each of the stronger ones of the septet units due to coupling with ^{105}Pd ($S = {}^5/_2$; natural abundance 22.2%). The following EPR parameters have been extracted: g = 2.065, $A(^{31}P) = 75.8 \times 10^{-4}$ cm^{-1}, $A(^{105}Pd) = 7.6 \times 10^{-4}$ cm^{-1} at 293 K; $g_{//} = 2.059$, $g_\perp = 2.078$, $A_{//}(^{31}P) = 88.8 \times$

(9) Gauthron, I.; Mugnier, Y.; Hierso, K.; Harvey, P. D. *Can. J. Chem.* **1997**, *75*, 1182.
(10) *CRC Handbook of Chemistry and Physics*, 64th ed.; CRC Press.: Boca Raton, FL, 1983; pp D−159.
(11) Strauss, S. H. *Chem. Rev.* **1993**, *93*, 927.

10^{-4} cm^{-1}, $A_{\perp}(^{31}P) = 85.0 \times 10^{-4}$ cm^{-1} at 100 K. The relative magnitude of the A constants ($A(^{31}P) \gg A(^{105}Pd)$) is due to the difference in the gyromagnetic ratio.[12] The presence of coupling with the Pd and P atoms is completely consistent with the atomic contributions of the SOMO (a_2). Indeed, previous EHMO computations on the Pd_3^{2+} species indicated that this MO is primarily composed of in-plane Pd d orbitals (d_{xy}, $d_{x^2-y^2}$ with minor p_x and p_y contributions) and some phosphorus components (p_y and p_x lone pairs), forming Pd−Pd and Pd−P antibonding MOs.[13]

Previous DFT calculations on geometry optimization predicted that the Pd−Pd distances are 2.592, 2.734, and 3.008 Å for Pd_3^{2+}, Pd_3^{+}, and Pd_3^{0}, respectively.[9] The former value is in agreement with X-ray data (2.604(30) Å),[7d,14] while the latter one is consistent with the $d^{10}-d^{10}-d^{10}$ electronic configuration and the distance found in the zerovalent $Pd_2(dppm)_3$, 2.959(2) Å.[15] The value of 2.734 Å for the Pd_3^{+} cluster indicates not only weak Pd−Pd bonding but also an increase in cavity size above the Pd_3 plane, suggesting that a larger substrate can penetrate inside this pocket.[16]

Carbon−Halogen Bond Activation with Electrochemical Induction. The Pd_3^{2+}, as a $CF_3CO_2^-$ salt, is unreactive toward most R−X substrates (X = Cl, Br, I) in stoichiometric quantities. However, the reaction can be electrochemically induced to form quantitatively the highly stable inorganic product $Pd_3(X)^+$ as identified by the comparison of the ^{31}P NMR and CV data of authentic samples.[17]

Interestingly, as shown in Table 1, the amount of electricity necessary to complete the conversion, as measured by coulometry (electrolysis at −0.48 V vs SCE), is not stoichiometric, being intermediate between 0 and 1 F/mol of cluster and depending upon the nature and relative excess of R−X (see the following).

To elucidate the organic coproducts derivated from the alkyl part of R−X, a series of experiments has been designed using benzyl halides $PhCH_2X$ (X = Br, I), which are potentially apt to form low-volatility GC/MS analyzable products. Starting from $PhCH_2Br$ (experiment 12 in Table 1, $Q = 0.80$ F/mol of cluster), we observed that the electrolyzed solution analysis provided evidence for the formation of $PhCH_2CH_2Ph$ (roughly estimated yield, 50%), $PhCH_3$ (not quantified as its peak is not fully resolved from that of the solvent), and $PhCH_2F$ (traces).

This set of products demonstrates that both the radical R$^{\bullet}$ and the carbocation R^+ are involved in the overall process. Indeed, $PhCH_2CH_2Ph$ must arise from homocoupling of $PhCH_2^{\bullet}$ and $PhCH_3$ from solvent hydrogen abstraction [THF has been reported earlier to act as a hydrogen donor]. On the other hand, the formation of $PhCH_2F$ witnesses the intermediacy of $PhCH_2^+$, which abstracts an F^- from the supporting electrolyte anion, PF_6^-. Supplemental evidence for the species "R^+" is provided by trapping with phenol, which gives the corresponding ether R−O−Ph and H^+.[6,18]

Table 1. Consumed Q for Electrochemically Induced RX Activation

entry	RX	molar ratio RX/cluster[a]	Q (F/mol of cluster)
1	$H_2C{=}CH{-}CH_2I$	1.1	thermal
2	CH3I	10	0.18
		1.1	0.39
3	CH_2I_2	1.1	0.45
4	C_2H_5I	1.1	0.72
5	$PhCH_2I$	1.1	0.20
6	$(CH_3)_3CI$	1.1	0.16
7	*n*-BuI	1.1	0.81
8	$PhCH_2CH_2I$	1.2	0.70
9	PhI	1.1	1.01
10	$(CH_3)_3CBr$	1.5	0.86
11	*n*-BuBr	1.1	no reactivity
12	$PhCH_2Br$	1.1	0.80
13	Me_2CHBr	1.1	no reactivity
14	$H_2C{=}CH{-}CH_2Br$	1.1	0.65
15	*n*-BuCl	1.1	no reactivity
		10	
16	$H_2C{=}CH{-}CH_2Cl$	1.1	0.80
17	*t*-BuCl	1.1	no reactivity
		10	

[a] All experiments started from $[Pd_3(dppm)_3(CO)(CF_3CO_2)](CF_3CO_2)$; however, for several RX, we have verified that Q does not significantly change when replacing PF_6^- by $CF_3CO_2^-$.

To explain the formation of R$^{\bullet}$ and R^+, one can conceive that two reactions compete, one leading to the radical and the other to the carbocation according to

$$Pd_3(L)^+ + R{-}X \rightarrow Pd_3(X)^+ + L^- + R^+ \quad (7)$$

$$Pd_3(L)^+ + R{-}X + e^- \rightarrow Pd_3(X)^+ + L^- + R^{\bullet} \quad (8)$$

where $L^- = CF_3CO_2^-$.[19]

As observed experimentally, the number of injected e^- is less than 1 per molecule of cluster (see Table 1), being directly related to its own part of reaction 7 in the consumption of $Pd_3(L)^+$. In accordance with our assumption, when $PhCH_2I$ is used instead of $PhCH_2Br$ with a considerably lower amount of electricity (0.2 against 0.8 F/mol, see Table 1), GPC/SM analysis shows that $PhCH_2F$ becomes the major product (yield, 86%) and $PhCH_2CH_2Ph$, the minor one (only traces detected).

Finally, the simultaneous appliance of reactions 7 and 8 can be explained by the fully detailed mechanism shown in Scheme 1. After the reduction step a, $Pd_3(L)^0$ dissociates into Pd_3^+ and L^- (step b). Previous studies have shown that, in the reduced

(12) The NMR frequencies in MHz at a 7.0463 T field are 121.442 for ^{31}P and 13.728 for ^{105}Pd in Drago, R. S. *Physical Methods for Chemists*, 2nd ed. Saunders College Publishing: Montreal, 1992. These data are also consistent with those found for $Rh_2(O_2CEt)_4(PPh_3)^{2+}$ as an example: $A_{//}(^{31}P) = 205 \times 10^{-4}$ cm^{-1}; $A_{\perp}(^{31}P) = 152 \times 10^{-4}$ cm^{-1}; $A_{//}(^{103}Rh) = 13 \times 10^{-4}$ cm^{-1}; $A_{\perp}(^{103}Rh)$ = not resolved in Kawamura, T.; Fukamachi, K.; Sowa, T.; Hayashida, S.; Yonezawa, T. *J. Am. Chem. Soc.* **1981**, *103*, 364.

(13) Harvey, P. D.; Provencher, R. *Inorg. Chem.* **1993**, *32*, 61.

(14) Provencher, R.; Harvey, P. D. *Inorg. Chem.* **1996**, *35*, 2113.

(15) Kirss, R. U.; Eisenberg, R. *Inorg. Chem.* **1989**, *28*, 3372.

(16) Zhang, T.; Drouin, M.; Harvey, P. D. *J. Chem. Soc., Chem. Commun.* **1996**, 877.

(17) The complexes have been prepared according to literature methods,[8] and the ^{31}P NMR and electrochemical data are as follow: δ (acetone-d_6) = −1.25 (PF_6^-), −7.01 ($CF_3CO_2^-$), −6.53 (Cl^-), −6.14 (Br^-), and −6.40 ppm (I^-); $E_{1/2}^{2+/0} = -0.77$ V (Cl^-), −0.68 V (Br^-), and −0.77 V (I^-) in THF solutions containing 0.2 M Bu_4NPF_6.

(18) As a representative example, Me_3CI was reacted with $Pd_3(CF_3CO_2)^+$ in a 1:1 ratio in a THF solution containing 0.2 M Bu_4NPF_6 as supporting electrolyte and PhOH (in the same molar amount as Me_3CI). After electrolysis, the solution was evaporated and the residue was extracted with Et_2O. The Ph−O−CMe_3 ether coupling product is detected in low yield by GC/MS (isolated yield = 25%). The low yield is due to inefficient trapping of the unstable carbocation for this stoichiometric reaction.

(19) As stated previously, the starting material $Pd_3(CF_3CO_2)^+$ exists as a host−guest system where the $CF_3CO_2^-$ substrate is held by $Pd_3^{2+}\cdots CF_3CO_2^-$ electronic interactions inside the cavity based upon X-ray data.[7d] The binding constant found for carboxylates are relatively weak with respect to anion species but strong with respect to neutral organic molecules.

Scheme 1

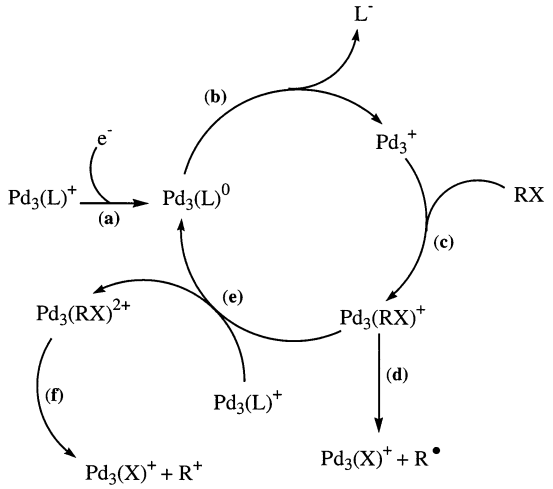

state, the binding of L^- is no more stabilizing.[20] So, the R−X substrate is able to penetrate into the empty cavity of the Pd_3^+ cluster to form the host−guest complex $Pd_3(RX)^+$ (step c). Hence, there are two reaction possibilities: (i) the activated R−X undergoes a C−X homolytic cleavage to form the radical R• and $Pd_3(X)^+$ (step d); (ii) alternatively, a solution outer-sphere electron transfer (SET) occurs between $Pd_3(RX)^+$ and $Pd_3(L)^+$, which gives $Pd_3(RX)^{2+}$ and $Pd_3(L)^0$ (step e). The latter is able to enter in a new catalytic cycle, and the former forms the carbocation through the heterolytic cleavage of the C−X bond (step f). There is no direct evidence (e.g., spectroscopic proof) of the extremely reactive $Pd_3(RX)^{2+}$. However, the same intermediate type is demonstrated to exist and to react strictly in the same way within the reactivity of Pd_3^{2+} onto acid chlorides (see the following).

To demonstrate the reasonability of steps c and d of Scheme 1, a slight excess of $PhCH_2Br$ was added to a pure solution of Pd_3^+: an immediate reaction took place, leading quantitatively to $Pd_3(Br)^+$ and to PCH_2CH_2Ph (44%) and $PhCH_3$, with no R^+ forming product, that is, $PhCH_2F$.

Reaction 7 is made of steps b + c + e. The ET step a initiates the catalytic sequence, allowing for the quick elimination of L^-, which is blocking the cluster reactive site.[19] In that way, the reaction with R−X is rendered faster. We have found that reaction 7 can operate solely, without electrochemical induction, but over longer periods of time (typically, 1 day is necessary for the reaction between the cluster and $PhCH_2Br$ to be completed, in comparison with 1 h for the electrocatalyzed method); accordingly, in the uncatalyzed conditions, $PhCH_2F$ is the only organic product observed (yield, 90%).

By injecting a small amount of electricity (0.04 F/mol for 1.1 equiv of substrate MeI for instance and stopping the electrolysis before the current reaches zero), we observe that the R−X activation reaction goes to completion after 1 h. As a result, the turnover number for this specific example becomes 24 (i.e., (1−0.04)/0.04) in comparison with 1.5 (i.e., (1−0.39)/0.39) for the more rapid exhaustive nonstop electrolysis (Table 1, entry 2). So, the turnover number is a function of the initial amount of injected electricity. In addition, as the substrate concentration increases, Q decreases which is consistent with the increased rate of reactivity.

Since the paramagnetic Pd_3^+ species is a potential reducing agent, quenching experiments were also investigated. The electrochemical generation of Pd_3^+ followed by the addition of 1 equiv of ferricinium (Fc^+) with no applied potential leads to the rapid formation of Pd_3^{2+} and ferrocene (Fc), as identified by RDE voltammetry, both in the presence and in the absence of R−X. The reactivity is explained by an outer-sphere electron transfer according to

$$Pd_3^+ + Fc^+ \rightarrow Pd_3^{2+} + Fc^0 \qquad (9)$$

The Fc^+/Fc couple is +0.56 V versus SCE in our experiments.

As stated in Table 1, Q varies as I < Br < Cl where most R−Cl substrates are found unreactive. For instance the allyl halides ($H_2C{=}CH{-}CH_2X$) require 0 (thermal), 0.65, and 0.80 F/mol for X = I, Br, and Cl, respectively. Similarly, the *n*-BuX substrates are unreactive for X = Br and Cl, and Q = 0.81 F/mol for X = I. This trend is consistent with the relative C−X bond strength.[21] The rare example of activated R−Cl substrates (i.e., $H_2C{=}CH{-}CH_2Cl$) stems from the charge stabilization by resonance in $H_2C{=}CH{-}CH_2^+$.

While a correlation between Q and the C−X bond strength is obvious such as for *i*-PrBr (no reactivity), *n*-BuBr (no reactivity), $PhCH_2Br$ (Q = 0.80 F/mol, 1.1 equiv), and *t*-BuBr (Q = 0.86 F/mol, 1.5 equiv), for instance, other comparisons are not so direct. Indeed, Q for MeI is significantly smaller than Q for RCH_2CH_2I (R = H, Et, Ph), the latter values being similar. In fact, the smaller MeI substrate interacts more efficiently with the Pd_3^+ center inside the phenyl-dppm cavity than the longer RCH_2CH_2I substrates. In addition, the Q value for *t*-BuI is small despite its size and reflects the relative stability of the carbocation Me_3C^+ and the reduced probability of a back reaction ($R^+ + X^- \rightarrow R{-}X$; inductive effect). This observation is also corroborated by the PhI datum, where no charge stabilization is effective. Indeed Q = 1.01 F/mol, a maximum value where the turnover number of 1 is obtained (i.e., stoichiometric). In this case, the carbocation Ph^+ is a strong Lewis acid, and a back reaction is very efficient.

Thermally Induced R−X Activation. On some occasions, the $Pd_3(CF_3CO_2)^+$ species exhibits slow thermal R−X activation. The time scale for the thermal activation ranges from hours to days under stoichiometric conditions, in comparison with ~15 min in the electrochemical induced studies. This reactivity becomes faster as the quantity of substrate becomes more important. This is due to the host−guest behavior of the $CF_3CO_2^-$ anion, which can be displaced by a higher amount of substrate, allowing substrate·····Pd_3^{2+} interactions without electrochemical induction. The thermal reactivity can be monitored by UV−vis spectroscopy where the starting inorganic material, Pd_3^{2+}, and the final product, $Pd_3(X)^+$, exhibit λ_{max} at 496 or 484 nm (PF_6^- and $CF_3CO_2^-$ as counteranions) and 464 nm, for $X^- = Cl^-$, Br^-, and I^-, respectively. Figure 3 shows a typical example of the progression of the UV−vis spectra with time during an R−X activation reaction (R−X = *n*-BuI).

(20) Lemaître, F.; Brevet, D.; Lucas, D.; Vallat, A.; Mugnier, Y.; Harvey, P. D. *Inorg. Chem.* **2002**, *41*, 2368.

(21) March, J. *Advanced Organic Chemistry*; John Wiley and Sons: New York, 1992; p 24.

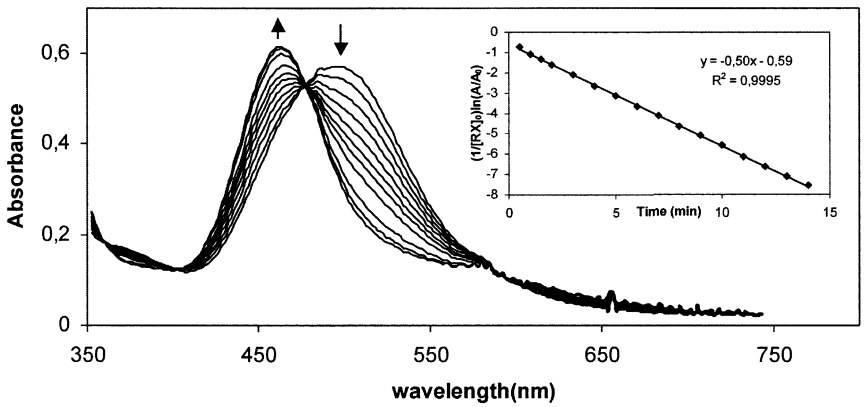

Figure 3. UV−vis spectral changes during the reaction between Pd_3^{2+} (2.78×10^{-5} M) and 1000 equiv of BuI in THF.

Experimentally, it has been found that the reaction rate (v) can be expressed as in eqs 10 and 11 (details provided in the Supporting Information):

$$v = k[\mathrm{RX}][\mathrm{Pd_3}^{2+}] \quad (\text{counteranion} = \mathrm{PF_6}^-) \qquad (10)$$

$$v = k^* \frac{[\mathrm{RX}][\mathrm{Pd_3(L)}^+]}{[\mathrm{L}^-]} \quad (\text{counteranion} = \mathrm{L}^- = \mathrm{CF_3CO_2}^-) \qquad (11)$$

This result is consistent with the fact that $CF_3CO_2^-$ blocks the cavity, whereas, with PF_6^-, it can be considered free to access for the R−X substrate.[16,19]

When a large excess of R−X is used (typically, a 1000-fold excess), eqs 10 and 11 can be simplified to

$$v = k[\mathrm{RX}]_0[\mathrm{Pd_3}^{2+}] \quad (\text{counteranion} = \mathrm{PF_6}^-) \qquad (12)$$

$$v = k^* \frac{[\mathrm{RX}]_0[\mathrm{Pd_3(L)}^+]}{[\mathrm{L}^-]} \quad (\text{counteranion} = \mathrm{L}^- = \mathrm{CF_3CO_2}^-) \qquad (13)$$

where $[RX]_0$ is the concentration at $t = 0$.

From eqs 12 and 13, one can demonstrate that the rate constant k or k^* can be obtained according to (Supporting Information)

$$\frac{1}{[\mathrm{RX}]_0} \ln \frac{[\mathrm{Pd_3}^{2+}]}{[\mathrm{Pd_3}^{2+}]} = -kt \quad (\text{counteranion} = \mathrm{PF_6}^-) \qquad (14)$$

$$\frac{[\mathrm{Pd_3(L)}^+]_0}{[\mathrm{RX}]_0}\left(2 \ln \frac{[\mathrm{Pd_3(L)}^+]}{[\mathrm{Pd_3(L)}^+]_0} + 1 - \frac{[\mathrm{Pd_3(L)}^+]}{[\mathrm{Pd_3(L)}^+]_0}\right) = -k^*t \quad (\text{counteranion} = \mathrm{L}^- = \mathrm{CF_3CO_2}^-) \qquad (15)$$

The inset of Figure 3 shows an example of such an analysis, and the data are compared in Tables 2 and 3. Numerous important trends are noticed. First, the rates vary as Cl < Br < I for a given substrate, illustrating further the effect of the C−X bond strength on the rates. Finally in the *n*-alkane series, the rate also varies according to *n*-BuI < *n*-PrI < EtI < MeI, suggesting a small effect of steric hindrance on the rates, while the C−I bond strength remains relatively constant along this group. This trend was also observed with the Q values extracted in the electrochemically induced activation.

Table 2. Rate Constants for the R−X Activation by $Pd_3(CF_3CO_2)^+$ in a 1000:1 Ratio

RX	$10^6 \times k^*$ (min^{-1})
t-BuI	instantaneous
n-BuI	1.48
n-PrI	3.02
EtI	5.52
MeI	6.40
t-BuBr	1.35
$H_2C{=}CH{-}CH_2I$	instantaneous
$H_2C{=}CH{-}CH_2Br$	2.75
$H_2C{=}CH{-}CH_2Cl$	1.73

Table 3. Rate Constants for the R−X Activation by Pd_3^{2+} in a 1000:1 Ratio

RX	k ($L\ mol^{-1}\ min^{-1}$)
t-BuI	instantaneous
n-PrI	0.842
MeI	0.853
n-BuI	0.50

Table 4. Rate Constants for the *t*-BuI Stoichiometric Activation by $Pd_3(L)^+$

L^-	experimental conditions	$10^3 \times k^*$ (min^{-1})
$CF_3CO_2^-$		5.24
$CF_3CO_2^-$	+1 equiv Ag^+	5.34
$CF_3CO_2^-$	+0.2 M $(TBA)PF_6$	5.49
$CF_3CO_2^-$	+1 equiv Tl^+	4.75

L^-	k ($mol\ L^{-1}\ min^{-1}$)
PF_6^-	instantaneous

Many substrates react so fast at this level of [RX] that k cannot be measured. This is the case for *t*-BuI where instantaneous reactions are observed upon mixing the Pd_3^{2+} and R−X solutions, for ratios 1:1000 and 1:100. However, for 1:10 with $Pd_3(CF_3CO_2)^+$, the reaction becomes slow enough for analysis. The *t*-BuI substrate has been investigated in a little more detail in the stoichiometric conditions (i.e., for a 1:1 ratio). While it still reacts spontaneously with $Pd_3(PF_6)^+$ (i.e., the cavity is available), the slower reaction for the $Pd_3(CF_3CO_2)^+$ case allows (Table 4) the rate constant k^* to be extracted from (see Supporting Information)

$$\ln \frac{[\mathrm{Pd_3(L)}^+]}{[\mathrm{Pd_3(L)}^+]_0} + 2\frac{[\mathrm{Pd_3(L)}^+]_0}{[\mathrm{Pd_3(L)}^+]} - 2 = k^*t \qquad (16)$$

The addition of 0.2 M Bu_4NPF_6 (typical concentration in the electrochemical activation) or 1 equiv of Ag^+ or Tl^+ does not change greatly the rate within the experimental uncertainty. These observations indicate that the R−X activations are not influenced by the presence of the supporting electrolyte and that Pd_3^{2+} must be a much stronger Lewis acid than Ag^+ (under stoichiometric conditions).

Acid Chloride Activation. In a stoichiometric amount, RCOCl reacts with $Pd_3(L)^+$ ($L^- = CF_3CO_2^-$, PF_6^-) without electrochemical induction. This reactivity has been monitored by CV and ^{31}P NMR. Thus, the presence of $Pd_3(Cl)^+$ has been clearly demonstrated as the sole inorganic product. As a typical example, Figure 4 shows the progression of the CV of a $Pd_3(CF_3CO_2)^+$ solution in the presence of 1 equiv of RCOCl (R = *t*-Bu) where the electrochemical system of the initial cluster (A/A′) is gradually replaced by that of the chloride adduct (B/B′). So, the reaction proceeds according to

$$Pd_3(L)^+ + RCOCl \rightarrow Pd_3(Cl)^+ + L^- + \text{“}RCO^+\text{”} \quad (17)$$

$$R = t\text{-Bu, Ph, } CH_3\text{, } Me_2CH\text{, } n\text{-}C_6H_{13}$$

$$L^- = CF_3CO_2^-,\ PF_6^-$$

The presence of the “RCO^+” intermediate (R = Ph for instance) has been demonstrated by trapping it with anisole to form the corresponding *p*-methoxybenzophenone according to

$$PhC{=}O^{\oplus} + PhOCH_3 \xrightarrow{-H^+} Ph\text{-}\underset{\underset{O}{\|}}{C}\text{-}C_6H_4(OCH_3) \quad (18)$$

The low amount of the starting material used does not allow deduction of the chemical yield precisely in stoichiometric conditions.

Two mechanisms are possible. The associative mechanism involves a host−guest intermediate between the Pd_3^{2+} cluster and the nondissociated RCOCl molecule. This mechanism is described by the following equations:

$$Pd_3(L)^+ \underset{k_{-1}}{\overset{k_1}{\rightleftharpoons}} Pd_3^{2+} + L^- \quad (19)$$

$$Pd_3^{2+} + RCOCl \underset{k_{-2}}{\overset{k_2}{\rightleftharpoons}} Pd_3^{2+}\cdots\cdots Cl(CO)R \quad (20)$$

$$Pd_3^{2+}\cdots\cdots Cl(CO)R \xrightarrow{k_3} Pd_3(Cl)^+ + \text{“}RCO^+\text{”} \quad (21)$$

This mechanism is essentially the same as that observed in the alkyl halide cases. However, a dissociative mechanism must also be considered, due to the weaker bonding C−Cl interactions in the RCOCl molecules. The equations are as follows:

$$RCOCl \underset{k_{-2}'}{\overset{k_2'}{\rightleftharpoons}} \text{“}RCO^+\text{”} + Cl^- \quad (22)$$

$$Pd_3^{2+} + Cl^- \xrightarrow{k_3'} Pd_3(Cl)^+ \quad (23)$$

where the Pd_3^{2+} is also generated according to eq 19. In the case where $L^- = PF_6^-$, the $Pd_3(L)^+$ cluster is completely dissociated in solution and eq 19 does not apply. Thus, when

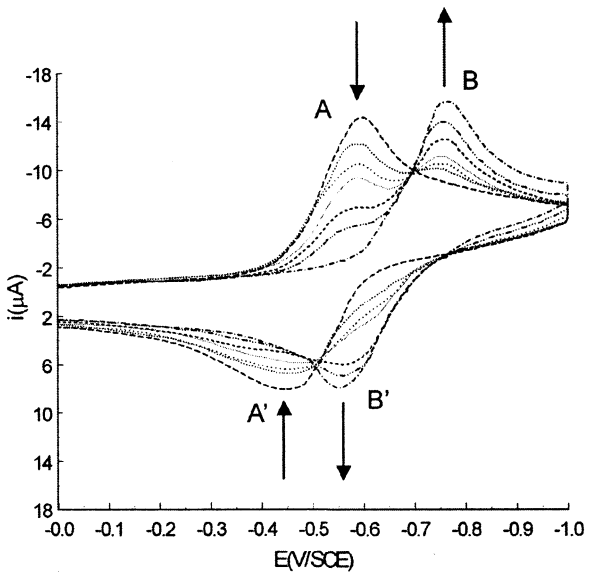

Figure 4. Cyclic voltammogram evolution of $Pd_3(CF_3CO_2)^+$ (0.5 mM) with 1 equiv of *t*-BuCOCl in THF with 0.2 M NBu_4PF_6. Initial potential: 0 V. Scan rate: 100 mV s^{-1}.

the dissociative mechanism is applied, the theorical rate law is as follows (Supporting Information):

$$v = -\frac{d[RCOCl]}{dt} = \frac{k_2'k_3'[Pd_3^{2+}][RCOCl]}{k_{-2}'[RCO^+] + k_3'[Pd_3^{2+}]} \quad (24)$$

At the beginning of the reaction, $k_{-2}'[RCO^+] \ll k_3'[Pd_3^{2+}]$ and the rate can be expressed as

$$v = k_2'[RCOCl] \quad (25)$$

The rate constant k_2' can be obtained according to

$$\ln\frac{[RCOCl]}{[RCOCl]_0} = -k_2't \quad (26)$$

With both clusters, from an analysis of the time-resolved CV, the linearity of the graphs $\ln([RCOCl]/[RCOCl]_0)$ versus time (for R = Ph, *t*-Bu) indicates a dissociative mechanism (see, as an example, Figure 5b). The data were also analyzed assuming the associative mechanism, but did not lead to a linear behavior with the corresponding equations (Figure 5a). The case of pivaloyl chloride is shown (Figure 6) for $Pd_3(L)^+$, where $L^- = CF_3CO_2^-$, PF_6^-. After a certain time, the data deviate from linearity, since the approximation $k_{-2}'[RCO^+] \ll k_3'[Pd_3^{2+}]$ no longer holds. The range of linearity is greater in the PF_6^- graph than that of $CF_3CO_2^-$. Indeed, in the latter case, $[Pd_3^{2+}]$ is controlled in part by the $Pd_3(CF_3CO_2)^+$ dissociation equilibrium (19):

$$[Pd_3^{2+}] = \frac{k_1[Pd_3(L)^+]}{k_{-1}[L^-] + k'_3[Cl^-]} \quad (27)$$

In fact, at any time, $[Pd_3^{2+}]$ is lower than in the PF_6^- case, and in this way, the previous approximation is valid upon a shorter period of reaction time.

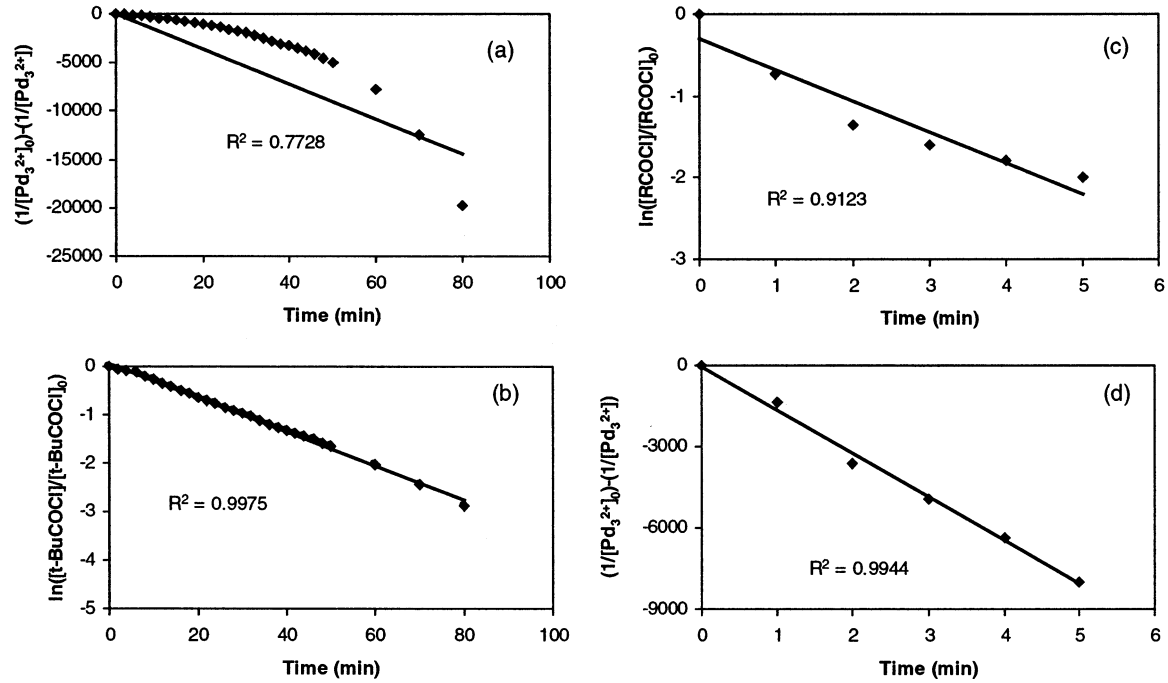

Figure 5. First-order plot for the reactivity of Pd_3^{2+} ($[Pd_3^{2+}]_0 = 0.8$ mM) with 1 equiv of *t*-BuCOCl (b) or $Me_2CHCOCl$ (c); variation of $\ln([RCOCl]/[RCOCl]_0)$ as a function of time. Second-order plot for the reactivity of Pd_3^{2+} ($[Pd_3^{2+}] = 0.8$ mM) with 1 equiv of *t*-BuCOCl (a) or $Me_2CHCOCl$ (d); variation of $(1/[Pd_3^{2+}]_0)-(1/([Pd_3^{2+}])$ as a function of time.

Table 5. Solvent Effect on the Kinetic Constant for the Reaction between $Pd_3(CF_3CO_2)^+$ and *t*-BuCOCl

solvent	k'_2 (min^{-1})
THF	0.038
CH_2Cl_2	0.057
acetone	0.253

The solvent effect on the rate (Table 5) indicates an increase in rate with the polarity. These results support the dissociative mechanism.[22]

For the RCOCl substrates where R is an alkyl group (R = Me, Et, Pr, Me_2CH, *n*-C_6H_{13}), the kinetic data show rather that an associative mechanism operates. In this case, the general equation for the rate of reaction is (Supporting Information):

$$v = \frac{k_2 k_3 [Pd_3^{2+}][RCOCl]}{k_{-2} + k_3} = k[Pd_3^{2+}][RCOCl] \quad (28)$$

In the simplest case (counterion = PF_6^-; mechanism made of steps 20 and 21) and under stoichiometric conditions (ratio $[Pd_3^{2+}]_0/[RCOCl]_0 = 1/1$), integration of eq 28 leads to (Supporting Information)

$$\frac{1}{[Pd_3^{2+}]} - \frac{1}{[Pd_3^{2+}]_0} = kt \quad (29)$$

The corresponding plot for the above listed R groups (see Figure 5d for example) exhibits linearity, and the observed rate constant varies according to *n*-C_6H_{13} < *I*−Pr < Pr < Et < Me (Table 6). If a dissociative process is assumed, the inductive electron donation from R suggests that *n*-C_6H_{13} should dissociate more easily than Me, and so on. Accordingly, the reaction with the former must be faster. The rates indicate the reverse, suggesting that the larger the R group, the slower the reaction is, in agreement with a sterically sensitive associative process.

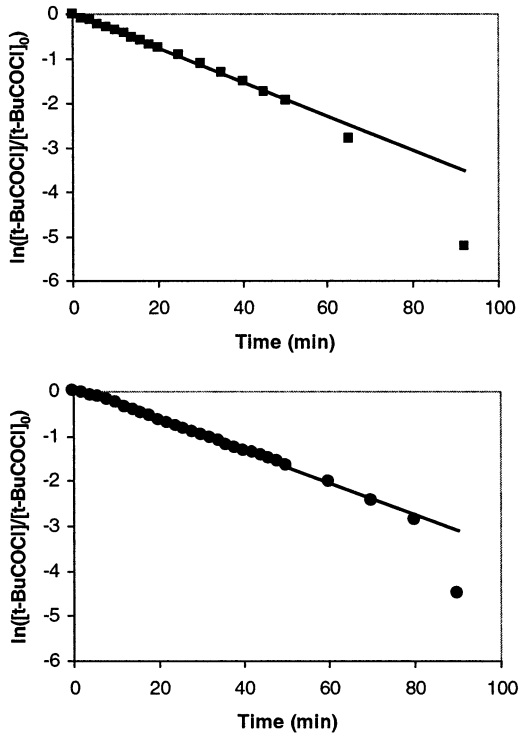

Figure 6. First-order plot for the reactivity of $Pd_3(CF_3CO_2)^+$ ($[Pd_3(CF_3CO_2)^+]_0 = 8 \times 10^{-4}$ mol/L) with 1 equiv of *t*-BuCOCl. Variation of $\ln([RCOCl]/[RCOCl]_0)$ as a function of time (top). First-order plot for the reactivity of Pd_3^{2+} ($[Pd_3^{2+}]_0 = 8 \times 10^{-4}$ mol/L) with 1 equiv of *t*-BuCOCl. Variation of $\ln([RCOCl]/[RCOCl]_0)$ as a function of time (bottom).

Design of a Catalytic Cycle. To render the RCOCl activation catalytic, one has to regenerate the starting Pd_3^{2+} catalyst by abstracting the chloride cleanly and irreversibly. The obvious

(22) March, J. *Advanced Organic Chemistry*; John Wiley and Sons: New York, 1992; p 450.

Table 6. Rate Constants for the Reaction between Pd_3^{2+} and RCOCl in the Associative Mode

RCOCl	k (L mol^{-1} min^{-1})
MeCOCl	3448
$Me(CH_2)_2COCl$	1609
$Me_2CHCOCl$	683
EtCOCl	2279
$CH_3(CH_2)_5COCl$	460

Scheme 2

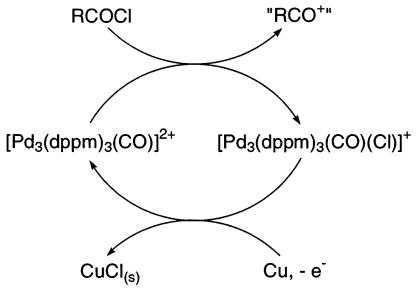

options are the precipitations of CuCl and AgCl by using the corresponding M(I) salts. The use of Cu(I) species to abstract Cl^- ions from polynuclear complexes is not uncommon.[23] Indeed, the Cl^- abstraction proceeds quantitatively according to

$$Pd_3(Cl)^+ + Ag^+ \xrightarrow{\text{slow}} Pd_3^{2+} + \underline{AgCl} \quad (30)$$

$$Pd_3(Cl)^+ + Cu(NCMe)_4^+ \longrightarrow Pd_3^{2+} + \underline{CuCl} + 4MeCN \quad (31)$$

where the counteranion is PF_6^- or BF_4^-.

The precipitation of CuCl and AgCl constitutes the driving force of the reaction. The cost of the Ag^+ reagent, however, motivates a cheaper alternative. In addition, the $Cu(NCMe)_4^+$ material requires its synthesis[24] prior to use. Instead, in a more practical way, this Cl^- abstraction reaction (eqs 30 and 31) can also proceed quantitatively in one step by means of an electrolysis using a copper anode. Indeed, the electrolysis of a $Pd_3(Cl)^+$ solution in CH_2Cl_2 with a copper anode as a working electrode operating at +0.65 V versus SCE leads to the desired reactivity (where the Pd_3^{2+} product is identified by cyclic voltammetry and ^{31}P NMR):

$$Pd_3(Cl)^+ + Cu - e^- \longrightarrow Pd_3^{2+} + \underline{CuCl} \quad (32)$$

Coulometric measurements indicate that 1 F/mol of $Pd_3(Cl)^+$ ($n_{exp} = 1.06$ F/mol) is required to regenerate Pd_3^{2+}. When these equations are combined, a catalytic cycle can be now described in Scheme 2. The Pd_3^{2+} catalyst acts as a strong Lewis acid which abstracts Cl^- from RCOCl to generate the very reactive acylium "RCO^+" intermediate. The inorganic product $Pd_3(Cl)^+$ diffuses toward the polarized copper anode, and a Cl^- ion transfer occurs to form CuCl at the surface, hence regenerating the Pd_3^{2+} catalyst. As a blank experiment, these same reactions were investigated in the absence of the Pd_3^{2+} species. In these cases, no current and no reactivity was detected. All in all, the Pd_3^{2+} cluster acts as a halide transfer agent from the organic molecule to the electrode surface.

Hence the overall reaction can be written as follows:

$$RCOCl + Cu_{(s)} - e^- \xrightarrow{Pd_3^{2+}\,(cat.)} RCO^+ + CuCl_{(s)} \quad (33)$$

A typical catalytic conversion is now described. When the Pd_3^{2+} cluster is introduced (as a PF_6^- salt) into a solution containing an excess of 100 molar equiv of RCOCl where R = Ph, *t*-Bu, or *n*-C_6H_{13}, polarizing the copper electrode generates a strong current. This current drops to zero when a quantity of electricity nearly equivalent to the amount of RCOCl initially introduced has passed. The weight of CuCl precipitate collected gave a yield approaching 100%. This catalysis using an Ag anode also allows the generation catalytically of the acylium "RCO^+" ion but was not investigated in this work. The interactions between $Pd_3(X)^+$ and Ag^+ ($X^- = Cl^-$, Br^-, I^-) are described in the following.

Applications. Knowing the strong electrophilic nature of the "RCO^+" species, we believe this catalytic system can be of great utility in acylation reactions. Two synthetic applications are now presented. These are the synthesis of fluoroacids[25] and conversions of alcohols in esters via *O*-acylation.[26] These selected reactions are based upon the following justifications.

Acid fluorides find numerous important applications in organic synthesis.[25,27,28] Generally, acid fluorides are prepared from halide exchange with the corresponding acid chloride[29] with the use of a fluorinating agent such as KF,[30] KF/HF,[31] HF,[32] SbF_3,[33] BrF_3,[34] and ZrF_2.[35] These reactions require high

(23) (a) Braunstein, P.; Luke, A. *New J. Chem*. **1988**, *12*, 429. (b) Braunstein, P.; Luke, M. A.; Tiripicchio, A.; Camellini, M. *Angew. Chem., Int. Ed. Engl*. **1987**, *26*, 768.
(24) Kubas, G. J. *Inorg. Synth*. **1979**, *19*, 90.
(25) (a) Carpino, L. A.; Sadat-Aalaee, H. G.; Chao, H. G.; Deselms, R. H. *J. Am. Chem. Soc*. **1990**, 112, 9651. (b) Bertho, J. N.; Loffet, A.; Pinel, C.; Reuther, F.; Sennyey, G. *Tetrahedron Lett*. **1991**, *32*, 1303. (c) Wenschuh, H.; Beyermann, M.; Krause, E.; Brudel, M.; Winter, R.; Schümann, M.; Carpino, L. A.; Bienert, M. *J. Org. Chem*. **1994**, *59*, *3275*.
(26) Carey, F. A.; Sundberg, R. J. *Advanced Organic Chemistry*, 3rd ed.; Plenum Press, 1990; Vol. I, p 475.
(27) (a) Ramig, K.; Kudzma, L. V.; Lessor, R. A.; Rozov, L. A. *J. Fluorine Chem*. **1999**, *94*, 1 and the references therein. (b) Hudlicky, M.; Pavlath, A. E. *Chemistry of Organic Fluorine Compounds II: A Critical Review*; American Chemical Society: Washington, DC, 1995.
(28) (a) Wagner, R.; Wiedel, B.; Günther, W.; Görls, H.; Anders, E. *Eur. J. Org. Chem*. **1999**, 2383. (b) Hyatt, J. A.; Raynolds, P. W. *J. Org. Chem*. **1984**, *49*, 384.
(29) (a) Hasek, W. R.; Smith, W. C.; Engelhardt, V. A. *J. Am. Chem. Soc*. **1960**, *82*, 543. (b) Bloshchitsa, F. A.; Burmakov, A. I.; Kunshenko, B. V.; Alekseeva, L. A.; Yagupol'skii, L. M. *J. Org. Chem. USSR* (English Translation) **1985**, *21*, 1286. (c) Ritter, S. K.; Hill, B. K.; Odian, M. A.; Dai, J.; Noftle, R. E.; Gard, G. L. *J. Fluorine Chem*. **1999**, *93*, 73.
(30) (a) Saunders, S. *J. Chem. Soc*. **1948**, 1778. (b) Haszeldine, N. *J. Chem. Soc*. **1959**, 1084. (c) Pittman, A. G.; Sharp, D. L. *J. Org. Chem*. **1966**, *31*, 2316. (d) 18-crown-6 complex: Liotta, C. L.; Harris, H. P. *J. Am. Chem. Soc*. **1974**, *96*, 2250. (e) Ishikawa, N.; Kitazume, T.; Yamazaki, T.; Mochida, Y.; Tatsuno, T. *Chem. Lett*. **1981**, 761. (f) Tordeux, M.; Wakselman, C. *Synth. Commun*. **1982**, *12*, 513. (g) Clark, J. H.; Hyde, A. J.; Smith, D. K. *J. Chem. Soc., Chem. Commun*. **1986**, *10*, 791. (h) Liu, H.; Wang, P.; Sun, P. *J. Fluorine Chem*. **1989**, *43*, 429. (i) Krespan, C. G.; Dixon, D. A. *J. Org. Chem*. **1991**, *56*, 3915.
(31) (a) Olah G. A.; Kuhn, S.; Beke, S. *Chem. Ber*. **1956**, *89*, 862. (b) Miller, J.; Ying, O.-L. *J. Chem. Soc*., Perkin Trans. *2*, **1985**, 325.
(32) (a) Young, D. *J. Org. Chem*. **1959**, *24*, 1021. (b) Olah, G. A.; Welch, J. T.; Vankar, Y. D.; Nojima, M.; Kerekes, I.; Olah, J. A. *J. Org. Chem*. **1979**, *44*, 3872. (c) Abe, T.; Hayashi, E.; Baba, H.; Nagase, S. *J. Fluorine Chem*. **1984**, *25*, 419.
(33) Meerwein, H.; Borner, P.; Fuchs, O.; Sasse, H. J.; Schrodt, H.; Spille, J. Chem. Ber. **1956**, *89*, 2060.
(34) Rozen, S.; Ben-David, I. *J. Fluorine Chem*. **1996**, *76*, 145.
(35) (a) Blicke, F. F. *J.* Am. Chem. Soc. **1924**, *46*, 1516. (b) Swain, S. *J. Am. Chem. Soc*. **1953**, 75, 246. (c) Nenajdenko, V. G.; Lebedev, M. V.; Belenkova, E. S. *Tetrahedron Lett*. **1995**, *36*, 6317.

temperature which is rather inconvenient for polyfunctional systems. No catalyst is known for such a reaction.

In parallel, the conversion of alcohols into esters is of fundamental importance in organic synthesis.[26] The acylating agent may be the acid chloride or the corresponding anhydride as shown by eq 34:

$$RC(O)Y + R'(OH) \rightarrow RC(O)OR' + HY \qquad (34)$$
$$Y = Cl, OC(O)R$$

The most popular catalyst used for this reaction is 4-(dimethylamino)pyridine (DMAP), which needs the presence of a base, generally a tertiary amine.[36] The drawback is that the quantity of required catalyst is comparatively great (5−10%) instead of the 1% commonly used and the amine cocatalyst is in excess. In addition, DMAP is uneffective toward sterically hindered alcohols. Occasionally, high temperature, long reaction time, and excess of acyl reagents are necessary. This situation has led over the past 10 years to the development of various catalysts, including $TaCl_5$,[37] TMSOTf,[38] $Sc(OTf)_3$,[39] Bu_3P,[40] $CoCl_2$,[41] Montmorillonite K-10 and KSF,[42] and inorganic solids such as alumine[43] and zinc.[44]

The acid fluorides are prepared by using a fluorinated supporting electrolyte, that is, Bu_4NPF_6 or Bu_4NBF_4. Indeed, the catalytic conversion into acid fluoride operates readily and quantitatively from the corresponding acid chloride according to

$$RCOCl + F^- + Cu_{(s)} - e^- \xrightarrow[\substack{CH_2Cl_2 \\ 0.2\ M\ Bu_4NPF_6\ or\ Bu_4NBF_4}]{Pd_3^{2+}\ (1\%)} RCOF + CuCl_{(s)} \qquad (35)$$

The reaction is quasi-quantitative in faradaic yields, and high chemical yields are obtained according to GC−MS findings (Table 7), for all the acid chlorides (R = Ph, *t*-Bu, *n*-C_6H_{13}) and "F^-" donors. The proposed mechanism involves the abstraction of an F^- from the PF_6^- or BF_4^- anion by the strongly electrophilic "RCO^+" ion. Previous studies have demonstrated the ability of both anions to act as sources of F^- to fluorinate electrophilic centers, such as either organometallic[45] or even carbocationic groups.[46]

Table 7. Fluorination (Entries 1−4) and Alcoholysis (Entries 5−12) of Acid Chlorides Catalyzed by Pd_3^{2+} (1% mol) under Oxidation with a Copper Anode[f]

entry	acid chloride	nucleophile	Q[a] (F/mol)	chemical yield (%)	faradaic yield (%)
1	PhCOCl	Bu_4NPF_6	0.98	98	100
2	PhCOCl	Bu_4NBF_4	0.90	86	96
3	*t*-BuCOCl	Bu_4NBF_4	0.88	86	98
4	*n*-C_6H_{13}COCl	Bu_4NPF_6	0.89	86	97
5	PhCOCl	MeOH	0.88	84	95
6	PhCOCl	EtOH	0.84	78	93
7	*t*-BuCOCl	EtOH	0.85	80	94
8	*n*-C_6H_{13}COCl	EtOH	0.93	85	91
9	PhCOCl	*i*-PrOH	0.81	80	99
10	PhCOCl	*sec*-BuOH	0.84	80	95
11	PhCOCl	*t*-BuOH	0.86	0[d]	0[d]
12	PhCOCl	*t*-BuOH	0.81	78[e]	96[e]

[a] Determined per mol of RCOCl, after the current had dropped to zero; the nonstoichiometric amount of electricity (relative to the quantity of acid chloride) can be explained by the passivation of the copper anode which appears at the end of the electrolysis, recovered with cuprous chloride. [b] Determined by GC/MS (internal standard method). [c] Faradaic yield = chemical yield/*Q*. [d] No more ester was found when the same experiment was conducted with excess alcohol (10 equiv relative to PhCOCl). [e] Conducted in an undivided cell. [f] See the general procedure in the Experimental Section.

Similarly, the rapid and mild conversion of alcohols into esters proceeds by the same way with the exception that Bu_4NClO_4 is used as a nonreactive supporting electrolyte (the data are compared in Table 7):

$$RCOCl + R'OH + Cu_{(s)} - e^- \xrightarrow[\substack{CH_2Cl_2 \\ 0.2\ M\ Bu_4NPF_6\ or\ Bu_4NBF_4}]{Pd_3^{2+}\ (1\%)} RCO_2R' + CuCl_{(s)} + H^+ \qquad (36)$$

The reactions are found to be almost quantitative (faradaic yields close to 100%). Again the nature of R or the nucleophile (here aliphatic alcohols) does not play an important role on the efficiency of the reactions, even with sterically encumbered reagents such as pivaloyl chloride or *tert*-butyl alcohol.

Because reaction 36 releases H^+, a secondary process occurs such as the catalytic dehydration of the alcohols, as illustrated below:[47]

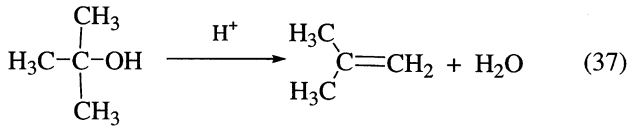

(37)

This undesired reactivity makes the ester preparation more unfavorable. To solve this problem, the use of a platinum cathode in the same compartment forces the reduction of H^+ as soon it is formed, thus giving the ester as the sole product (Table 7, entry 12). On the other hand, when the electrolysis proceeds in a double-compartment cell, the reaction does not produce the ester but rather the alkene and the acid (Table 7, entry 11).

$Pd_3(ClAg)^{2+}$ Intermediate. These processes are catalytic because the Cl^- ion is successfully and cleanly abstracted from the stable $Pd_3(Cl)^+$ inorganic product. The key intermediates in the catalytic cycle are the $Pd_3(ClM)^{2+}$ species (M = Cu, Ag). These unstable species in solution have been investigated and

(36) (a) Hofle, G.; Steglich, W.; Vorbruggen, H. *Angew.* Chem., Int. Ed. Engl. **1978**, *17*, 569. (b) Scriven, E. F. V. *Chem. Soc. Rev.* **1983**, *12*, 129.
(37) Chandrasekhar, S.; Ramachander, T.; Takhi, M. *Tetrahedron Lett.* **1998**, *39*, 3263.
(38) (a) Procopiou, P. A.; Baugh, S. P. D.; Flack, S. S.; Inglis, G. G. A. *Chem. Commun.* **1996**, 2625. (b) Procopiou, P. A.; Baugh, S. P. D.; Flack, S. S.; Inglis, G. G. A. *J. Org. Chem.* **1998**, *63*, 2342.
(39) (a) Ishihara, K.; Kubota, M.; Kurihara, H.; Yamamoto, H. *J. Am. Chem. Soc.* **1995**, *117*, 4413. (b) Ishihara, K.; Kubota, M.; Kurihara, H.; Yamamoto, H. *J. Org. Chem.* **1996**, *61*, 4560. (c) Ishihara, K.; Kubota, M.; Yamamoto, H. *Synlett* **1996**, 265. (d) Barett, A. G. M.; Braddock, D. C. *Chem. Commun.* **1997**, 351. (e) Zhao, H.; Pendri, A.; Greenwald, R. B. *J. Org. Chem.* **1998**, *63*, 7559.
(40) (a) Vedejs, E.; Diver, S. T. *J. Am. Chem. Soc.* **1993**, *115*, 3358. (b) Vedejs, E.; Benett, N. S.; Conn, L. M.; Diver, S. T.; Gingras, M.; Oliver, P. A.; Peterson, M. J. *J. Org. Chem.* **1993**, *58*, 7286.
(41) Iqbal, J.; Srivastava, R. R. *J. Org. Chem.* **1992**, *57*, 2001.
(42) (a) Li, A.-X.; Li, T.-S.; Ding, T.-H. *Chem. Commun.* **1997**, 1389. (b) Bhaskar, P. M.; Loganathan, D. *Tetrahedron Lett.* **1998**, *39*, 2215.
(43) Nagasawa, K.; Yoshitake, S.; Amiya, T.; Ito, K. *Synth. Commun.* **1990**, *20*, 2033.
(44) Yadav, J. S.; Reddy, G. S.; Suinivas, D.; Himabindu, K. *Synth. Commun.* **1998**, *28*, 2337.
(45) (a) Jordan, R. F.; Dasher, W. E.; Echols, S. F. *J. Am. Chem. Soc.* **1986**, *108*, 1718. (b) Bochmann, M.; Wilson, L. M. *Organometallics* **1987**, *6*, 2556. (c) Gorrell, I. B.; Parkin, G. *Inorg. Chem.* **1990**, *29*, 2452.
(46) Swain, C. R.; Rogers, R. J. *J. Am. Chem. Soc.* **1975**, *97*, 799.
(47) Kaiser, E. M.; Woodruff, R. A. *J. Org. Chem.* **1970**, *35*, 1198.

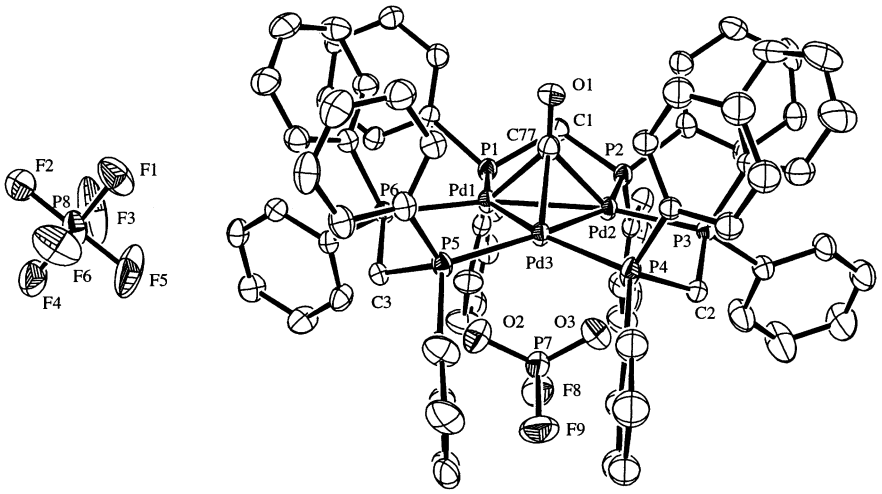

Figure 7. ORTEP drawing of $[Pd_3(dppm)_3(CO)(PF_2O_2)](PF_6)$. Toluene. The thermal ellipsoids are shown with 30% probability. The toluene solvation molecule and the H atoms are not shown for clarity.

tentatively isolated when possible. The $Pd_3(X)^+$ species reacts with $Cu(NCMe)_4^+$ and Ag^+ as stated for $X^- = Cl^-$ in eqs 31 and 32, according to

$$Pd_3(X)^+ + Cu(NCMe)_4^+ \longrightarrow Pd_3^{2+} + \underline{CuX} + 4\,MeCN \quad (38)$$

where $X^- = Cl^-$ and Br^- (with I^-, no reaction is seen within a day) and

$$Pd_3(X)^+ + Ag^+ \longrightarrow Pd_3^{2+} + \underline{AgX} \quad (39)$$

where $X^- = Cl^-$, Br^-, and I^-.

These reactions have been monitored by ^{31}P NMR where the starting and final products are clearly observed.[17] All the reactions are rapid where the signal of the desired $Pd_3(XM)^{2+}$ products is not observed, except for one case, $Pd_3(ClAg)^{2+}$. Indeed, this species exhibits a distinct ^{31}P signal at -4.65 ppm (s) which is intermediate between -1.25 (Pd_3^{2+}) and -6.53 ppm ($Pd_3(Cl)^+$). In addition, the solid-state IR spectrum shows a ν(CO) peak at 1820 cm^{-1}, which differs from ν(CO) in Pd_3^{2+} (1835 cm^{-1})[9] and $Pd_3(Cl)^+$ (1830 cm^{-1}). Finally, the FAB mass spectrum shows clear evidence for this species (details of the peak assignments are provided in the Supporting Information). The largest fragment is at the 1612.3 mass unit which corresponds to the fragment "$Pd_3(dppm)_3(ClAg)$" after the loss of CO. Bianchini et al. reported the structure of a complex which had some similarities with the $Pd_3(ClAg)^{2+}$ complex.[48] Indeed, Bianchini's compound, formulated as $[(PP_3)RuH(\eta^1\text{-}ClTl)](PF_6)$ ($PP_3 = P(CH_2CH_2PPh_2)_3$) and containing TlCl as a ligand, was obtained by reaction of Tl^+ with the corresponding chloride complex. Structurally, the Tl−Cl−Ru fragment is observed, where the Cl atom behaves as a bridging ligand. It is interesting to note that Tl^+···phenyl interactions are also observed in this complex. This feature brings in the idea that π-systems stabilize metal cations. In relevance with this work, some calix[4]arenes have also been shown to act as hosts for the ion Ag^+, with evidence of π-arene complexation as well.[49] In view of these studies, we tentatively propose for $Pd_3(ClAg)^{2+}$ a bonding arrangement with the Ag(I) bonded to the Cl atom coordinated to the trimetallic unit, with possibly a stabilizing contribution of the phenyl groups of the dppm,[49] but this hypothesis would need to be supported by a structure determination.

Unfortunately, attempts to obtain single crystals suitable for X-ray structure determination stubbornly failed. The long period of time necessary to grow crystals leads to the slow precipitation of AgCl, and two types of crystals have been isolated. One has been identified as the Pd_3^{2+} starting material. In the second one, the compound can be formulated as $[Pd_3(dppm)_3(CO)(PO_2F_2)](PF_6)$, which shows that, during the course of this study, an interesting side reaction occurred between the counteranion PF_6^- and the residual H_2O in the solvents (acetone/toluene/hexane) to form the $PF_2O_2^-$ anion as demonstrated from crystallography (Figure 7). This hydrolysis reaction is relatively scarce, as only a few other examples in the case of palladium complexes exist to our knowledge.[50] The authors of this original paper explained the formation of this $PF_2O_2^-$ anion from a complex scheme of reactions involving species such as POF_4^-, SiF_4 (from the SiO_2), and SiF_6^{2-}, according to

$$H_2O + PF_6^- \rightarrow POF_4^- + 2HF \quad (40)$$

$$SiO_2 + 4HF \rightleftharpoons SiF_4 + 2H_2O \quad (41)$$

$$SiF_4 + 2F^- \rightarrow SiF_6^{2-} \quad (42)$$

$$POF_4^- + H_2O \rightarrow PO_2F_2^- + 2HF \quad (43)$$

In this structure, the $PF_2O_2^-$ anion is located inside the cavity. Due to size, this anion is likely favored to penetrate the cavity over the larger PF_6^- anion,[7d] and one may speculate that this interaction could drive the reaction. The interactions between the $PF_2O_2^-$ anion and the Pd_3^{2+} center are electrostatic in nature, as the O···Pd distances are 2.718 and 2.930 Å. The values compare favorably to those reported for the related cluster $[Pd_3(dppm)_3(CO)(CF_3CO_2)](PF_6)$.acetone (2.75(2) and 2.68(2)

(48) Bianchini, C.; Masi, D.; Linn, K.; Mealli, C.; Peruzzini, M.; Anobini, F. *Inorg. Chem.* **1992**, *31*, 4036.

(49) For example, see: Xu, W.; Puddephatt, R. J. *Organometallics* **1994**, *13*, 3054.

(50) Fernandez-Galan, R.; Manzano, B. R.; Otero, A.; Lanfranchi, M.; Pellinghelli, M. A. *Inorg. Chem.* **1994**, *33*, 2309.

Table 8. Comparison of the $Pd_3(dppm)_3(CO)^{2+}$ Skeletons[a]

	d(Pd–Pd) Å	d(Pd–P) Å	d(Pd–C) Å	d(C═O) Å	ref
$[Pd_3(PF_2O_2)]PF_6$	2.612	2.322	2.104	1.17	this work
$[Pd_3(CF_3CO_2)]PF_6$	2.595	2.311	2.08	1.17	7d
$[Pd_3(Cl)]BF_4$	2.595	2.312	2.104	1.15	7c
$[Pd_3](PF_6)_2$	2.613	2.318	2.104	1.16	7d

[a] Averaged values.

Å). The bond length and angles (Supporting Information) are normal and compare favorably to those other $Pd_3(dppm)_3(CO)^{2+}$ species investigated in our laboratory (Table 8).[51] The comparison indicates that there are practically no changes in structure parameters upon host−guest interactions within the experimental uncertainties. This list includes the $Pd_3(Cl)^+$ species for which the binding constant is very large.[16,52] This behavior may reflect the soft−hard Lewis acid/base affinity properties of the Pd_3^{2+} centers and donors.

Attempts to abstract X^- from $Pd_3(X)^+$ ($X^- = Cl^-$, Br^-, I^-) with Tl^+ and abstract Cl^- from $Pd_3(Cl)^+$ with $AlCl_3$ have been made in CH_2Cl_2 and THF. No reaction was observed. On the other hand, the abstraction of Cl^- from $AlCl_4^-$ by the unsaturated Pd_3^{2+} species operates rapidly and quantitatively according to

$$Pd_3^{2+} + AlCl_4^- \rightarrow Pd_3(Cl)^+ + \text{“}AlCl_3\text{”} \qquad (44)$$

This result illustrates the stronger Lewis acidity of the Pd_3^{2+} in these solvents. Based upon this work's results, this reaction must proceed by a host−guest interaction between the $AlCl_4^-$ anion and the Pd_3^{2+} cluster similar to that indicated by the X-ray structure of the $Pd_3(PF_2O_2)^+$ species discussed previously, forming a "$Pd_3{\cdots}Cl{\cdots}AlCl_3^+$" intermediate, followed by a rapid Cl^- abstraction by the Pd_3^{2+} cluster. In comparison with the acid chlorides, allyl chlorides, and alkyl chlorides (here no reactivity), the rates of abstraction vary as $AlCl_4^- >$ RCOCl > allyl−Cl ≫ R−Cl and are consistent with the relative A−Cl bond strength (A = atom).

(51) (a) The term “host−guest“ complex is generally reserved for reversible systems.[51b] The halide adducts $Pd_3(X)^+$ do not exhibit such reversibility, and therefore, the use of this term is inappropriate in this case, even if the strongly coordinated X^- ions are located inside the cavity. (b) Connors, K. A. *Binding Constants: The Measurements of Molecular Complex Stability*; J. Wiley and Sons: New York, 1987.

(52) Harvey, P. D.; Hierso, K.; Braunstein, P.; Morise, X. *Inorg. Chim. Acta* **1996**, *250*, 337.

Conclusion

This work illustrated the C−X bond activation properties of the Pd_3^{2+} unsaturated cluster. Both bond strength and host−guest (guest sizes versus cavity dimension) interactions influence both the rate of reactivity and the mechanism. This species shows a better Lewis acid behavior than that “traditional” Lewis acids such as $AlCl_3$. The preparations of ethers, esters, and acid fluorides show the great potential for organic synthesis, particularly when the reaction is rendered catalytic. The elucidation of the intermediate $Pd_3(ClAg)^{2+}$ is very interesting. The use of such a Lewis acid opens the door to other applications such as catalytic nucleophilic substitution with inversion of configuration (SN_2) assisted by a transition metal and regioselective Friedel−Crafts reactions, operating within a constrained area above the Pd_3^{2+} plane. Further research will be published in due course.

Acknowledgment. P.D.H. thanks the NSERC (Natural Sciences and Engineering Research Council) and FCAR (Fonds Concertés pour l'Avancement de la Recherche) for funding. Y.M. is grateful to the CNRS (Centre National de la Recherche Scientifique) and Conseil Régional de Bourgogne for funds.

Supporting Information Available: Demonstration and integration of kinetic rate laws and their relations to mechanisms, peak assignments of the $Pd_3(dppm)_3(CO)(ClAg)^{2+}$ FAB mass spectrum, tables giving crystal data and details of the structure determination, atomic coordinates, bond distances, bond angles, anisotropic thermal parameters, and hydrogen atom positions for $[Pd_3(dppm)_3(CO)(PF_2O_2)](PF_6)$. This material is available free of charge via the Internet at http://pubs.acs.org.

JA0297786